Cell Reports, Volume *41*

Supplemental information

Acute depletion of human core nucleoporin reveals direct roles in transcription control but dispensability for 3D genome organization

Xiaoyu Zhu, Chuangye Qi, Ruoyu Wang, Joo-Hyung Lee, Jiaofang Shao, Lanxin Bei, Feng Xiong, Phuoc T. Nguyen, Guojie Li, Joanna Krakowiak, Su-Pin Koh, Lukas M. Simon, Leng Han, Travis I. Moore, and Wenbo Li

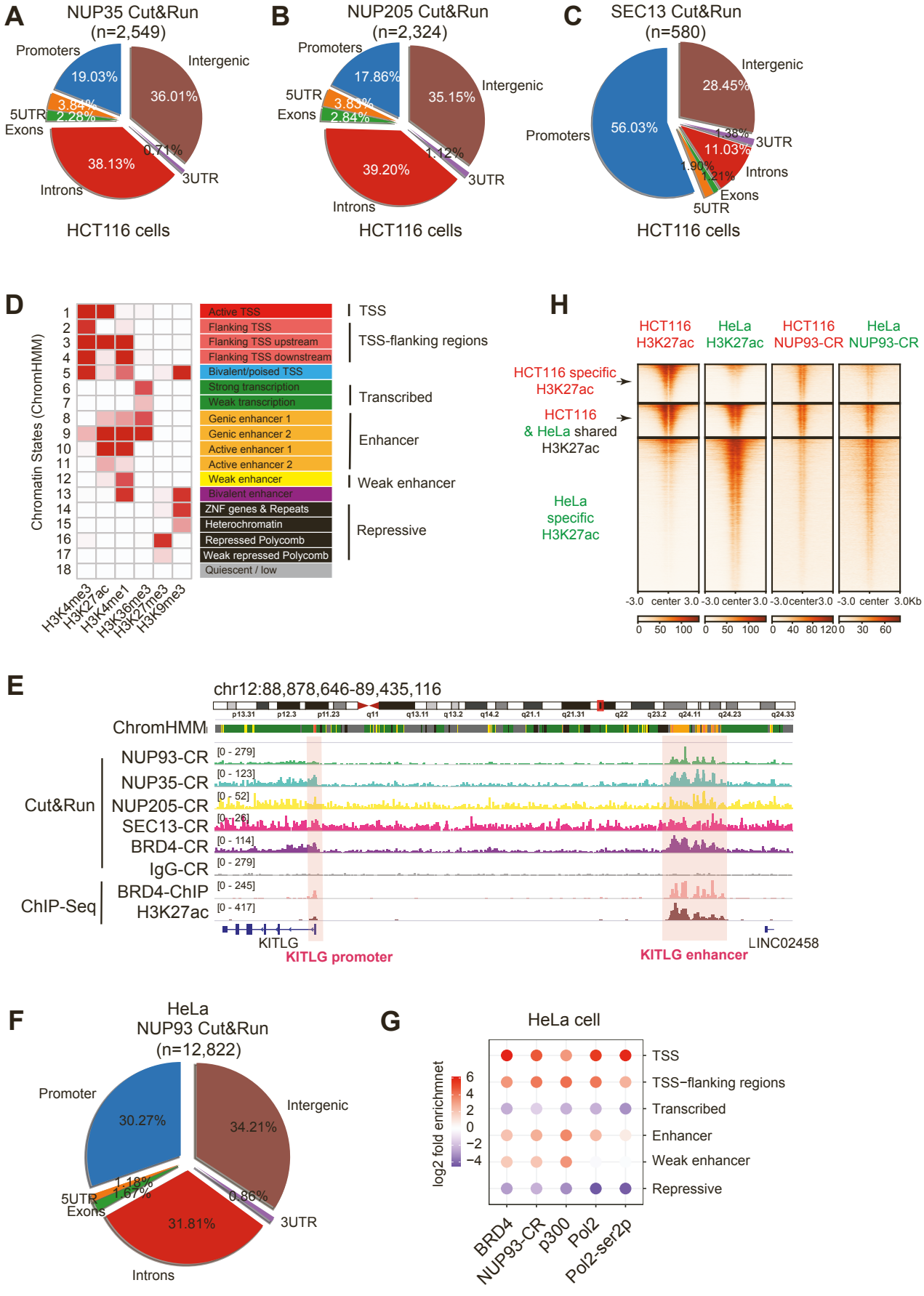
A
NUP35 Cut&Run
(n=2,549)
Promoters
19.03%
Intergenic
36.01%
5UTR
3.84%
Exons
2.28%
0.71%
38.13%
Introns
3UTR
HCT116 cells
B
NUP205 Cut&Run
(n=2,324)
Promoters
17.86%
Intergenic
35.15%
5UTR
3.83%
Exons
2.84%
1.12%
39.20%
Introns
3UTR
HCT116 cells
C
SEC13 Cut&Run
(n=580)
Intergenic
28.45%
Promoters
56.03%
1.38%
3UTR
11.03%
1.90%
1.21%
Introns
Exons
5UTR
HCT116 cells
D
Chromatin States (ChromHMM)
1
2
3
4
5
6
7
8
9
10
11
12
13
14
15
16
17
18
Active TSS
Flanking TSS
Flanking TSS upstream
Flanking TSS downstream
Bivalent/poised TSS
Strong transcription
Weak transcription
Genic enhancer 1
Genic enhancer 2
Active enhancer 1
Active enhancer 2
Weak enhancer
Bivalent enhancer
ZNF genes & Repeats
Heterochromatin
Repressed Polycomb
Weak repressed Polycomb
Quiescent / low
TSS
TSS-flanking regions
Transcribed
Enhancer
Weak enhancer
Repressive
H3K4me3
H3K27ac
H3K4me1
H3K36me3
H3K27me3
H3K9me3
H
HCT116
H3K27ac
HeLa
H3K27ac
HCT116
NUP93-CR
HeLa
NUP93-CR
HCT116 specific
H3K27ac
HCT116
& HeLa shared
H3K27ac
HeLa
specific
H3K27ac
-3.0 center 3.0
-3.0 center 3.0
-3.0center3.0
-3.0 center 3.0Kb
0 50 100
0 50 100
0 40 80 120
0 30 60
E
chr12:88,878,646-89,435,116
p13.31
p12.3
p11.23
q11
q13.11
q13.2
q14.2
q21.1
q21.31
q22
q23.2
q24.11
q24.23
q24.33
ChromHMM
Cut&Run
NUP93-CR
[0 - 279]
NUP35-CR
[0 - 123]
NUP205-CR
[0 - 52]
SEC13-CR
[0 - 26]
BRD4-CR
[0 - 114]
IgG-CR
[0 - 279]
ChIP-Seq
BRD4-ChIP
[0 - 245]
H3K27ac
[0 - 417]
KITLG
LINC02458
KITLG promoter
KITLG enhancer
F
HeLa
NUP93 Cut&Run
(n=12,822)
Promoter
30.27%
Intergenic
34.21%
5UTR
1.18%
Exons
1.67%
0.86%
31.81%
Introns
3UTR
G
HeLa cell
log2 fold enrichmnet
6
4
2
0
−2
−4
TSS
TSS−flanking regions
Transcribed
Enhancer
Weak enhancer
Repressive
BRD4
NUP93-CR
p300
Pol2
Pol2-ser2p

Figure S1. Core nucleoporins bind active promoters and enhancers with cell-type specificity (related to Figure 1).

(A-C) Peak distribution of NUP35, NUP205 and SEC13 Cut&Run within the 5′ UTR, Exon, Intron, 3′ UTR, promoter and intergenic regions.

(D) Chromatin ChromHMM states (18-state) defined on the basis of the observed data for six histone modifications (see **Table S2** and **Methods**). For each histone mark, the color intensity corresponds to the probability of observing that mark in the specific chromatin state. Candidate-state descriptions for each state, followed by a state abbreviation, are shown to the right.

(E) Genome browser tracks showing the binding of various NUPs and BRD4 Cut&Run (-CR) or ChIP-Seq at *KITLG* and *KITLG* enhancer regions.

(F) Peak distribution of NUP93 Cut&Run in HeLa cells within the 5′ UTR, Exon, Intron, 3′ UTR, promoter and intergenic regions.

(G) Similar to **Figure 1D**, this plot shows the enrichment of NUP93 and other factors in HeLa cells on specific chromatin states (we used annotated genome segmentation by ChromHMM in HeLa cells (Roadmap Epigenomics Consortium, 2015), see **Methods**).

(H) H3K27ac peaks at distal regions (TSSs ± 2kb were excluded) were divided into three groups based on cell type specificity: HCT116-specific (top row), HeLa-specific (bottom row), and shared peaks (middle row). Subsequently, normalized ChIP-Seq or Cut&Run (-CR) reads of H3K27ac or NUP93 centered at the middle of specific groups of H3K27ac peaks were plotted as heatmaps. Red labels used for HCT116 cells; green for HeLa cells.

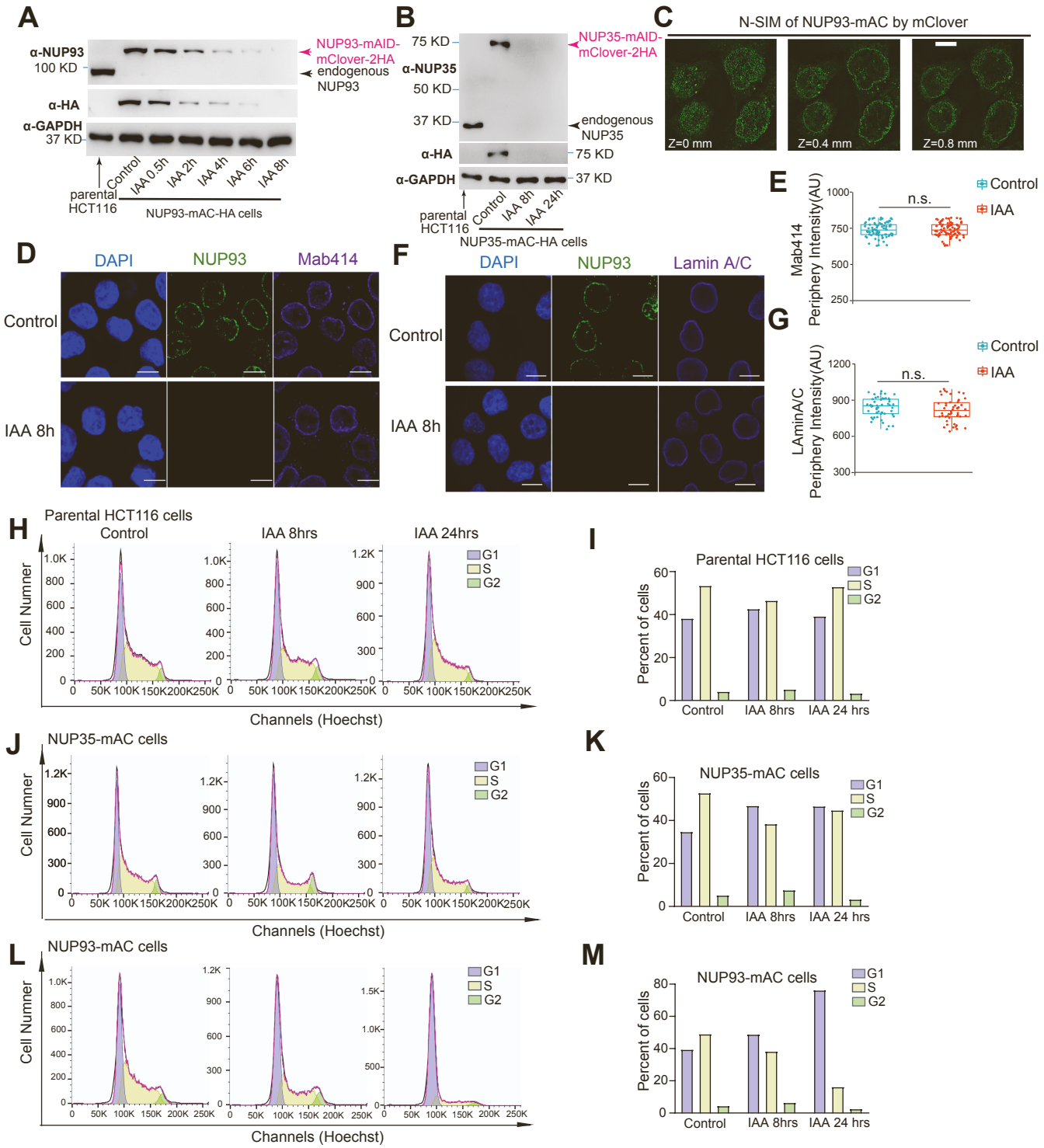
A
α-NUP93
100 KD
α-HA
α-GAPDH
37 KD
NUP93-mAID-mClover-2HA
endogenous NUP93
parental HCT116
Control
IAA 0.5h
IAA 2h
IAA 4h
IAA 6h
IAA 8h
NUP93-mAC-HA cells
B
75 KD
α-NUP35
50 KD
37 KD
α-HA
75 KD
α-GAPDH
37 KD
NUP35-mAID-mClover-2HA
endogenous NUP35
parental HCT116
Control
IAA 8h
IAA 24h
NUP35-mAC-HA cells
C
N-SIM of NUP93-mAC by mClover
Z=0 mm
Z=0.4 mm
Z=0.8 mm
D
DAPI
NUP93
Mab414
Control
IAA 8h
F
DAPI
NUP93
Lamin A/C
Control
IAA 8h
E
Mab414 Periphery Intensity(AU)
n.s.
Control
IAA
G
LAminA/C Periphery Intensity(AU)
n.s.
Control
IAA
H
Parental HCT116 cells
Control
IAA 8hrs
IAA 24hrs
Cell Numner
G1
S
G2
Channels (Hoechst)
I
Parental HCT116 cells
Percent of cells
Control
IAA 8hrs
IAA 24 hrs
J
NUP35-mAC cells
Cell Numner
Channels (Hoechst)
K
NUP35-mAC cells
Percent of cells
L
NUP93-mAC cells
Cell Numner
Channels (Hoechst)
M
NUP93-mAC cells
Percent of cells

Figure S2. Acute NUP93 and NUP35 depletion in human HCT116 cells (related to Figure 2).
(A) Western blots showing the protein levels of tagged NUP93-mAC-2HA after time course treatment by IAA, or the untagged NUP93 from the parental cells. Antibodies against NUP93 and HA tag were used to detect endogenous NUP93 protein. GAPDH was used as a loading control.
(B) Western blots showing the protein levels of tagged NUP35-mAC-2HA after IAA treatment for 8 hours or 24 hours, or untagged NUP35 in parental cells. Antibodies used are labeled in the panels. . GAPDH was used as a loading control.
(C) Structured illumination system (N-SIM) imaging of endogenous NUP93-mClover localization in the NUP93-mAC cells. Representative Z-sections at the nuclear membrane (Z = 0.0 μm), and at the nuclear interior (0.4 μm and 0.8 μm) are shown. Scale bar: 5 μm.
(D,E) Confocal images of NUP93-mAC cells stained by antibodies against NUP93 and Mab414 (a pan-NUP monoclonal antibody) in the presence or absence of NUP93 (Control or IAA 8hrs). Green: NUP93 with mClover. Blue: DAPI. Scale bars: 10μm. Panel E shows the quantification of Mab414 intensity in nuclear periphery; each dot represents the median fluorescence intensity in a cell (MFI, n>50, experiments done in duplicates). Student's T-tests, P values: ns, not significant.
(F,G) Similar to panels **D,E**, except that here the staining was done with a monoclonal antibody against LaminA/C.
(H,J,L) Cell cycle analysis was performed by flow cytometry of cells stained with Hoechst in parental HCT116, NUP35-mAC or NUP93-mAC cells after Vehicle treatment or IAA treatment for 8 and 24 hours. Cell cycle distribution and curve fitting were measured by FlowJo.
(I,K,M) Bar charts showing the percentages of cells distributed in different cell cycle phases for parental HCT116, NUP35-mAC or NUP93-mAC cells after Vehicle treatment (Control) or IAA treatment for 8 and 24 hours.

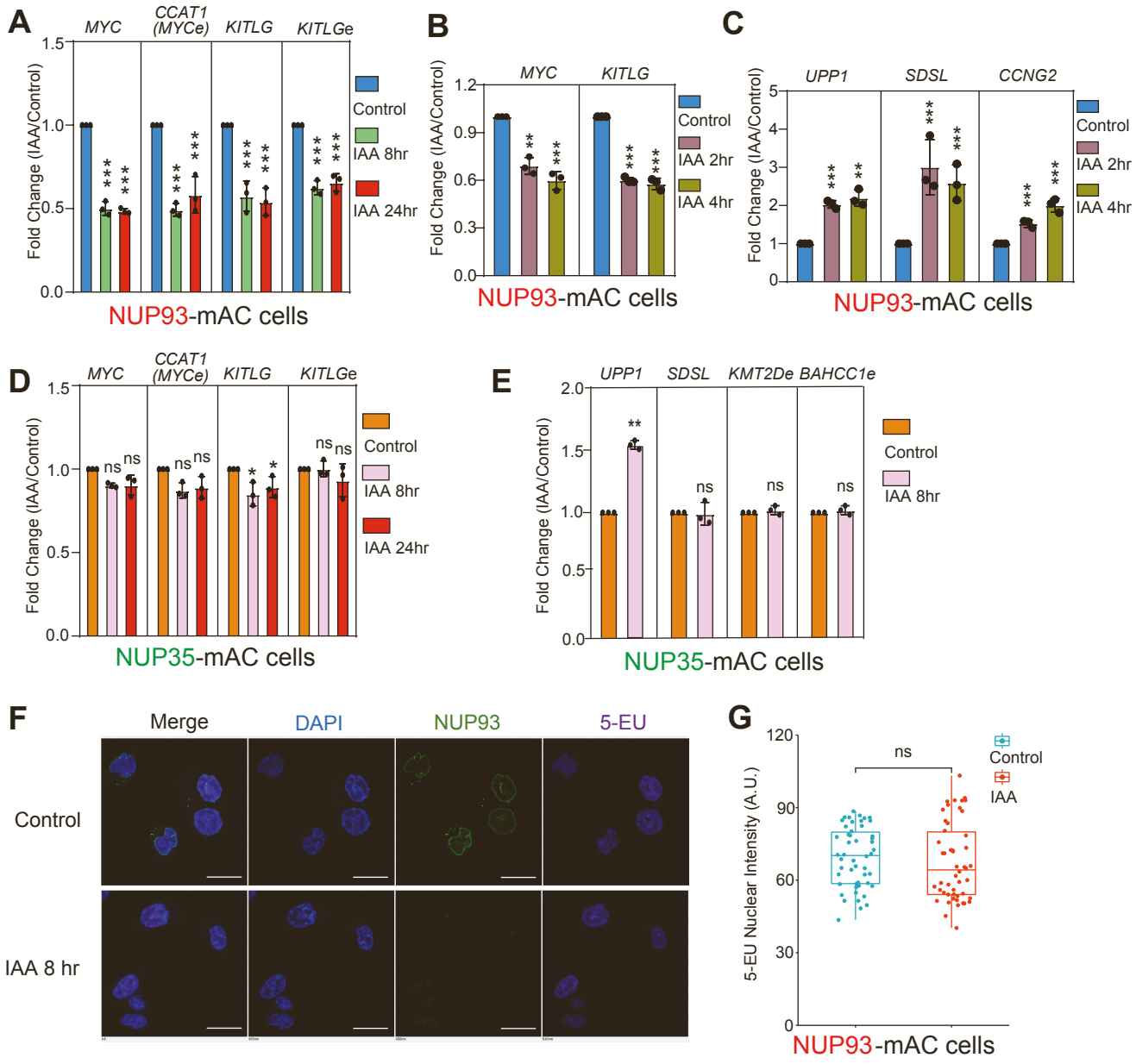
A
MYC
CCAT1 (MYCe)
KITLG
KITLGe
Fold Change (IAA/Control)
Control
IAA 8hr
IAA 24hr
NUP93-mAC cells
B
MYC
KITLG
Fold Change (IAA/Control)
Control
IAA 2hr
IAA 4hr
NUP93-mAC cells
C
UPP1
SDSL
CCNG2
Fold Change (IAA/Control)
Control
IAA 2hr
IAA 4hr
NUP93-mAC cells
D
MYC
CCAT1 (MYCe)
KITLG
KITLGe
Fold Change (IAA/Control)
Control
IAA 8hr
IAA 24hr
NUP35-mAC cells
E
UPP1
SDSL
KMT2De
BAHCC1e
Fold Change (IAA/Control)
Control
IAA 8hr
NUP35-mAC cells
F
Merge
DAPI
NUP93
5-EU
Control
IAA 8 hr
G
5-EU Nuclear Intensity (A.U.)
ns
Control
IAA
NUP93-mAC cells

Figure S3. Additional data on acute NUP93 and NUP35 depletion in human HCT116 cells (related to Figure 2).

(A) RT-qPCR analysis of gene expression after NUP93 acute depletion for two time points (8hrs or 24hrs after IAA treatment), showing alteration of genes and eRNAs to comparable levels.

(B) RT-qPCR analysis of NUP93-mAC cells after shorter time of IAA treatment (2hrs or 4hrs), showing that NDGs were already altered at these acute stages.

(C) Similar to panel **B**, but this shows expression of NSG genes after shorter term IAA treatments.

(D) RT-qPCR analysis of several genes and eRNAs in NUP35-mAC cells with or without IAA treatment for 8hrs or 24hrs showing no significant changes, except for slight reduction of *KITLG* mRNA.

(E) RT-qPCR analysis of several genes and eRNAs after IAA degradation of NUP35 (8hrs) in NUP35-mAC cells showing limited alteration, except a slight increase of *UPP1*. **A-E**, Bar graphs in panels **A-E** represent Mean ±SD (n=3 technical replicates). Each plot is a representative example from n=3 biological replicates. P values: Student's T-tests, *, $p < 0.05$; **, $p < 0.01$; ***: $p < 0.001$. N.S., not significant.

(F) Confocal images of example NUP93-mAC cells with/without IAA for 8hrs, showing comparable global transcription levels by 5-Ethynyl-uridine (5-EU) staining. 5-EU was added for 30 mins to measure de novo RNA synthesis in proliferating cells. Green: NUP93-mAC; purple: 5-EU staining. Blue: DAPI. Scale bars: 10μm.

(**G**) Box plot showing the quantification of 5-EU intensity in Control and IAA treated cells, each dot represents the median fluorescence intensity (MFI) in a cell. (n=50, experiments done in duplicates). Student's T-tests, P values: ns, not significant.

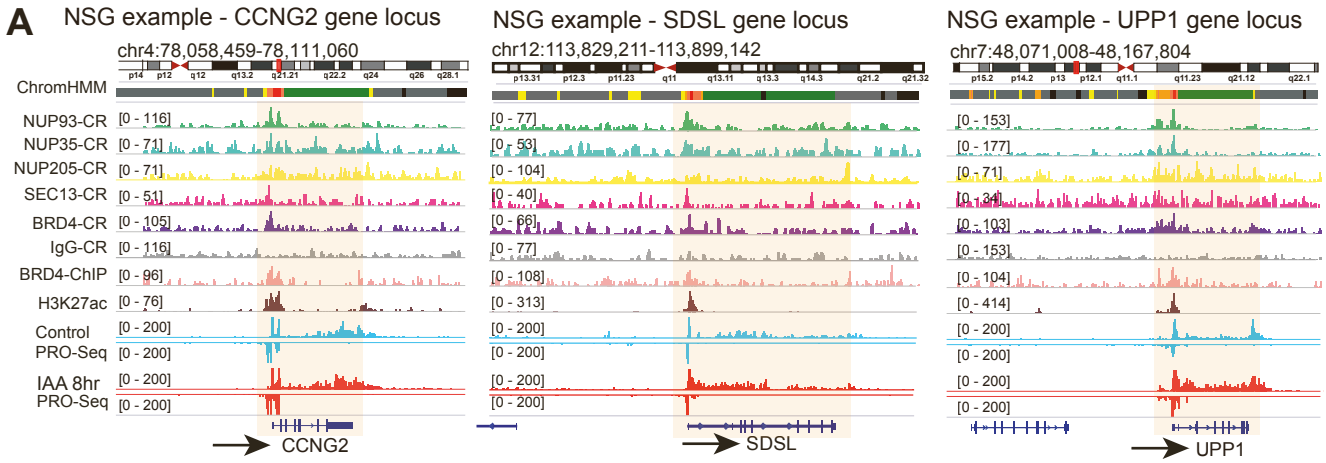
A
NSG example - CCNG2 gene locus
chr4:78,058,459-78,111,060
NSG example - SDSL gene locus
chr12:113,829,211-113,899,142
NSG example - UPP1 gene locus
chr7:48,071,008-48,167,804
ChromHMM
NUP93-CR
NUP35-CR
NUP205-CR
SEC13-CR
BRD4-CR
IgG-CR
BRD4-ChIP
H3K27ac
Control PRO-Seq
IAA 8hr PRO-Seq
CCNG2
SDSL
UPP1

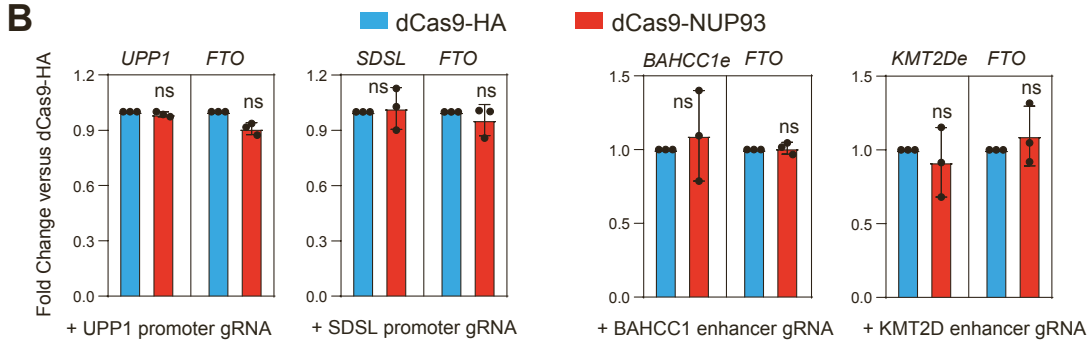
B
dCas9-HA
dCas9-NUP93
UPP1
FTO
SDSL
BAHCC1e
KMT2De
Fold Change versus dCas9-HA
ns
+ UPP1 promoter gRNA
+ SDSL promoter gRNA
+ BAHCC1 enhancer gRNA
+ KMT2D enhancer gRNA

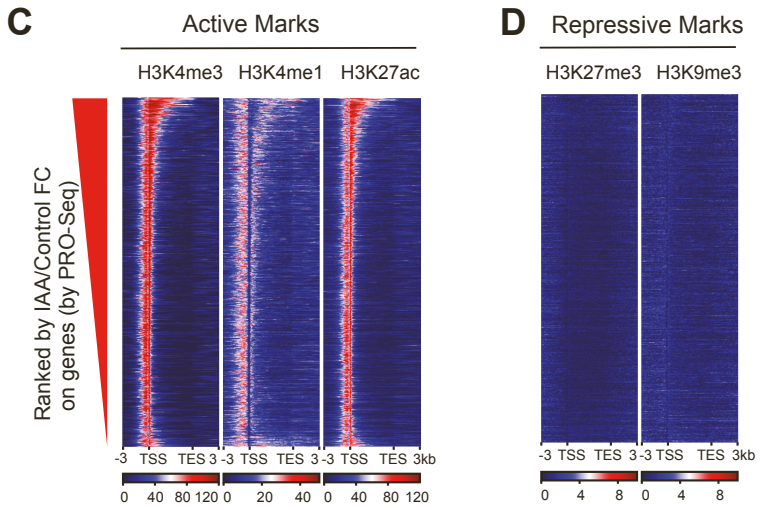
C
Active Marks
H3K4me3
H3K4me1
H3K27ac
Ranked by IAA/Control FC on genes (by PRO-Seq)
-3 TSS TES 3kb
D
Repressive Marks
H3K27me3
H3K9me3

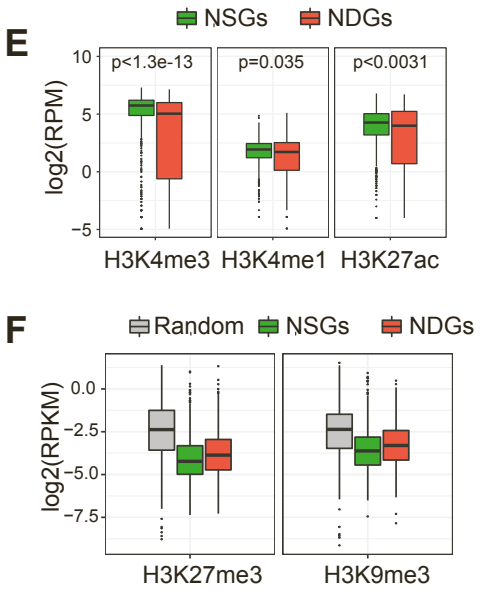
E
NSGs
NDGs
p<1.3e-13
p=0.035
p<0.0031
log2(RPM)
H3K4me3
H3K4me1
H3K27ac
F
Random
NSGs
NDGs
log2(RPKM)
H3K27me3
H3K9me3

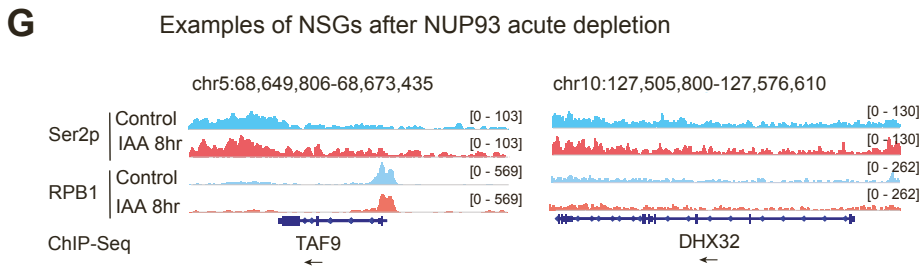
G
Examples of NSGs after NUP93 acute depletion
chr5:68,649,806-68,673,435
chr10:127,505,800-127,576,610
Ser2p
Control
IAA 8hr
RPB1
ChIP-Seq
TAF9
DHX32

Figure S4. dCas9 mediated NUP93 tethering to NSG genes and enhancers; additional chromatin features of NSGs and NDGs (related to Figures 3 and 4).

(A) Snapshot of genome browser tracks of Cut&Run (-CR) or ChIP-Seq of core NUPs, BRD4 and H3K27ac, and PRO-Seq tracks for Control and IAA conditions at several NSG loci. Highlighted areas denote NSG genes.

(B) RT-qPCR analysis of the expression of target genes upon CRISPR/dCas9 tethering of NUP93 to their promoters or enhancers (all data collected with IAA treatment for 8hr so the endogenous NUP93 was not present). Bar graph represents Mean ±SD (n=3 technical replicates). Each plot is a representative example from n=3 biological replicates. P values: Student's T-tests, *, $p < 0.05$. N.S., not significant. *FTO* gene mRNA was measured as a control.

(C,D) Heatmaps of the normalized ChIP-Seq reads of active histone marks (H3K4me3, H3K4me1 and H3K27ac in panel **C**) or repressive marks (H3K27me3 and H3K9me3 in panel **D**) on genes ranked by PRO-Seq fold change (IAA / Control). These were plotted the same way as **Figure 4C**.

(E) Boxplots showing ChIP-Seq intensity of H3K4me3, H3K4me1 and H3K27ac over the promoters of NSG versus NDG genes (related to panel **C**). P-values: Wilcoxon rank sum test.

(F) Boxplots showing ChIP-Seq intensity of H3K27me3 and H3K9me3 over gene bodies of three groups of genes: Random, NSGs and NDGs. "Random" indicates a random list of genes that are not transcribed.

(**G**) Snapshots of genome browser tracks of Pol2 and Ser2p ChIP-Seq in Control or IAA conditions over two example NSG genes; arrows indicate the direction of gene transcription.

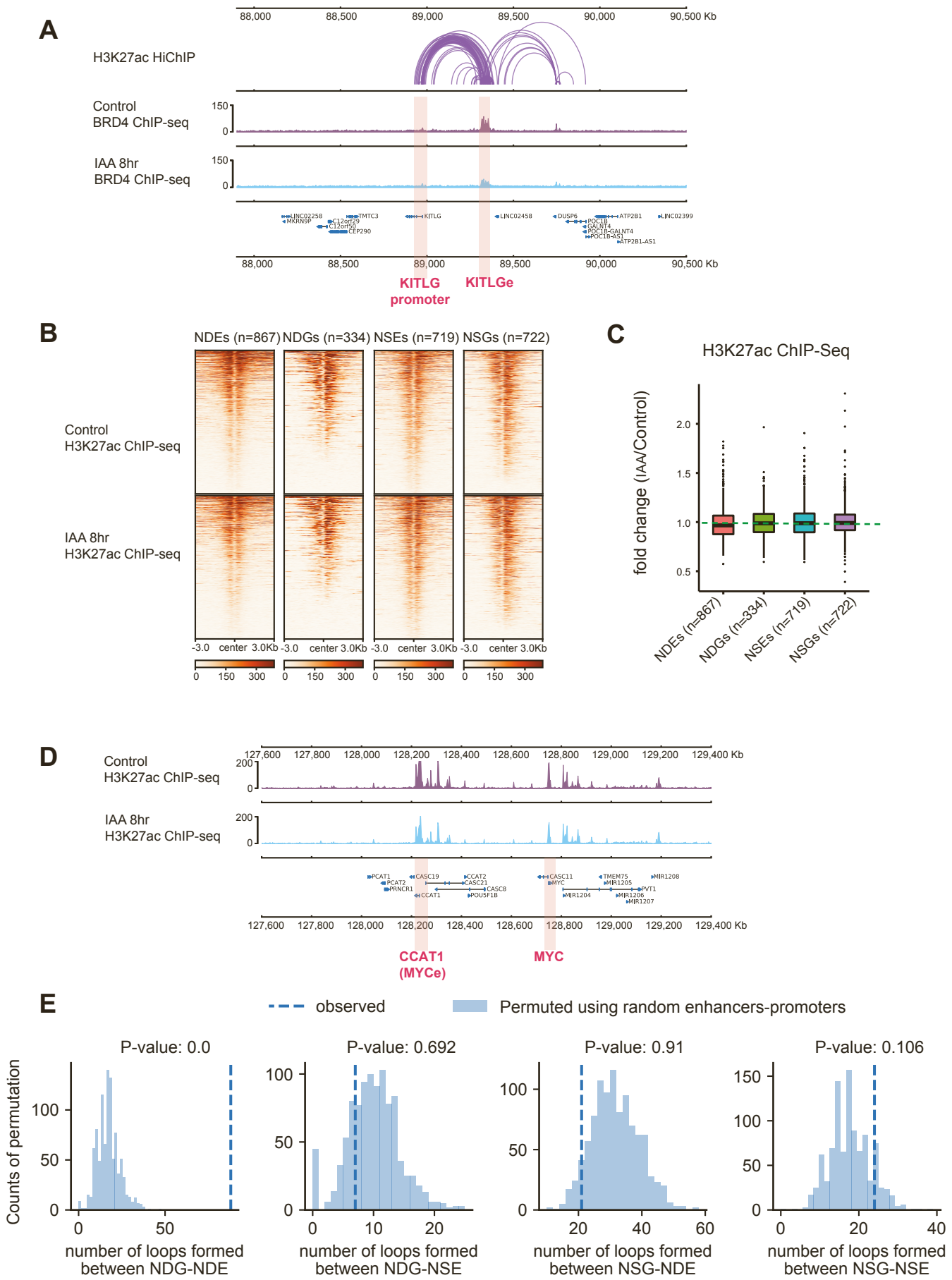
A
H3K27ac HiChIP
Control
BRD4 ChIP-seq
IAA 8hr
BRD4 ChIP-seq
88,000
88,500
89,000
89,500
90,000
90,500 Kb
KITLG
promoter
KITLGe
B
NDEs (n=867)
NDGs (n=334)
NSEs (n=719)
NSGs (n=722)
Control
H3K27ac ChIP-seq
IAA 8hr
H3K27ac ChIP-seq
-3.0
center
3.0Kb
C
H3K27ac ChIP-Seq
fold change (IAA/Control)
D
Control
H3K27ac ChIP-seq
IAA 8hr
H3K27ac ChIP-seq
127,600
127,800
128,000
128,200
128,400
128,600
128,800
129,000
129,200
129,400 Kb
CCAT1
(MYCe)
MYC
E
observed
Permuted using random enhancers-promoters
P-value: 0.0
P-value: 0.692
P-value: 0.91
P-value: 0.106
Counts of permutation
number of loops formed
between NDG-NDE
between NDG-NSE
between NSG-NDE
between NSG-NSE

Figure S5. Additional data on NUP93 regulated enhancers and promoters, and the lack of H3K27ac changes after NUP93 depletion (related to Figure 5).

(A) Genome browser tracks showing the data of H3K27ac HiChIP, BRD4 ChIP-seq and gene annotation coordinates. The *KITLG* gene and enhancer (*KITLGe*) are labeled. For H3K27ac HiChIP, each purple arch denotes a loop identified by FitHiChIP (Bhattacharyya et al., 2019).

(B) Heatmaps of H3K27ac ChIP-Seq on four groups of transcriptionally deregulated gene promoters or enhancers after NUP93 acute depletion (8hr IAA).

(C) Fold changes of H3K27ac ChIP-seq on four groups of transcriptionally deregulated gene promoters or enhancers after NUP93 acute depletion (8hr IAA), showing no significant difference.

(D) Genome browser showing similar H3K27ac signals at *MYC-MYCe* locus after NUP93 acute depletion (8hr IAA).

(E) Histograms showing the distributions of the "expected" numbers of H3K27ac HiChIP loops connecting randomly selected lists of promoters and enhancers that match the numbers of NDG-NDE, NDG-NSE, NSG-NDE, and NSG-NSE. Permutation was performed for 1,000 times using randomly shuffled enhancer-promoter pairs. Dash vertical line indicated the observed numbers of H3K27ac HiChIP loops in each category. P-values were calculated by the portion of permutation with expected numbers greater than observed numbers (related to **Figure 5G)**.

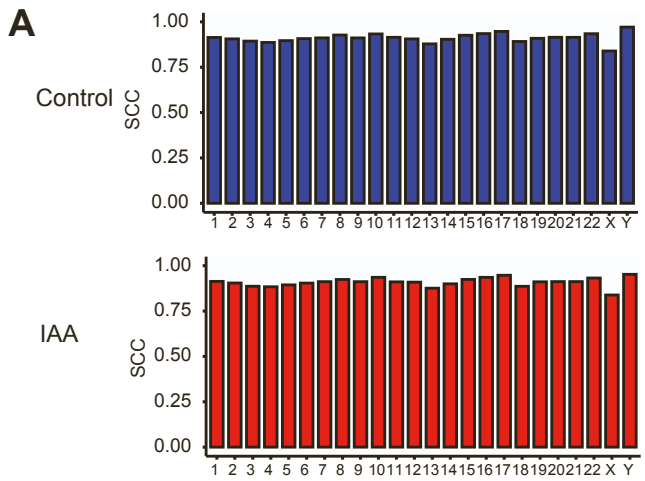
A
Control
IAA
SCC
1.00
0.75
0.50
0.25
0.00
1 2 3 4 5 6 7 8 9 10 11 12 13 14 15 16 17 18 19 20 21 22 X Y

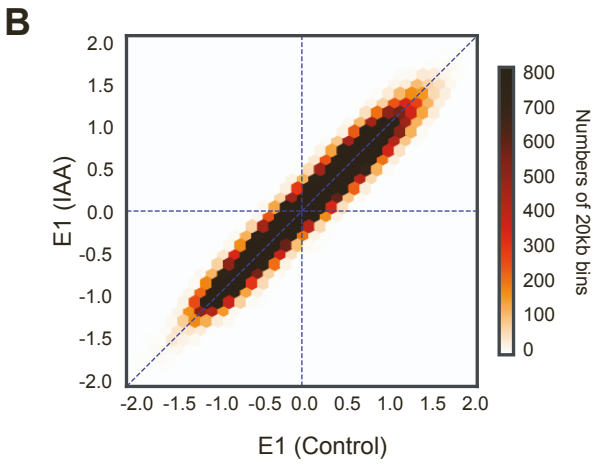
B
E1 (IAA)
E1 (Control)
2.0
1.5
1.0
0.5
0.0
-0.5
-1.0
-1.5
-2.0
Numbers of 20kb bins
800
700
600
500
400
300
200
100
0

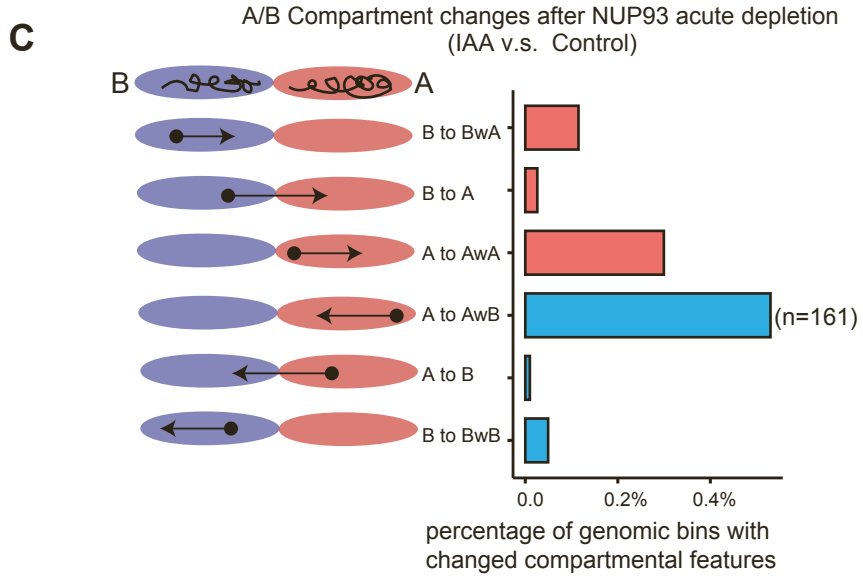
C
A/B Compartment changes after NUP93 acute depletion
(IAA v.s. Control)
B
A
B to BwA
B to A
A to AwA
A to AwB
A to B
B to BwB
(n=161)
0.0
0.2%
0.4%
percentage of genomic bins with
changed compartmental features

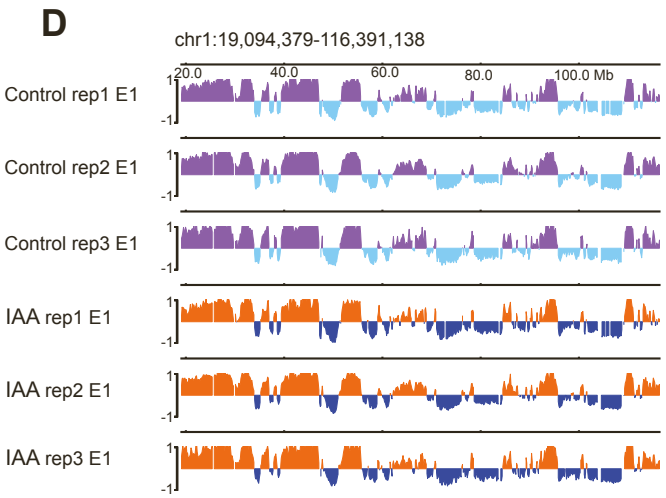
D
chr1:19,094,379-116,391,138
20.0
40.0
60.0
80.0
100.0 Mb
Control rep1 E1
Control rep2 E1
Control rep3 E1
IAA rep1 E1
IAA rep2 E1
IAA rep3 E1

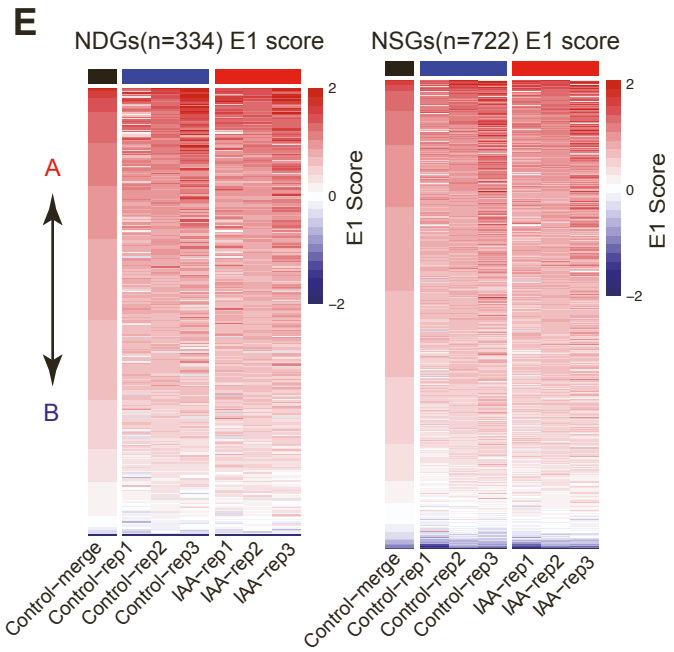
E
NDGs(n=334) E1 score
NSGs(n=722) E1 score
A
B
E1 Score
Control-merge
Control-rep1
Control-rep2
Control-rep3
IAA-rep1
IAA-rep2
IAA-rep3

Figure S6. Additional Hi-C data analysis showing overall unaltered 3D genome architecture after NUP93 acute depletion (related to Figure 6).

(A) Top and Bottom graphs showing stratum adjusted correlation coefficient (SCC) analyses between Hi-C replicates in Control and IAA (NUP93 acute depletion) conditions across different chromosomes, respectively.

(B) Scatter plot showing the correlation between E1 values of Hi-C data in Control (*x*-axis) versus IAA conditions (*y*-axis) by using principal component analysis (PCA) at 20 kb resolution.

(C) A diagram shows the analyses of A/B compartmental shifting (100 kb resolution, total bin numbers: 30,971) after acute NUP93 depletion (IAA 8hr v.s. Control). Diagram was adapted from Yusufova et al., 2020 (see **Methods**). Red and blue bars represent chromatin decompaction (E1 value increase) and compaction (E1 value decrease), respectively (BwA: shift within compartment B to a higher E1 value; AwA: shift within compartment A to a higher E1 value; AwB: shift within compartment A to a smaller E1 value; BwB: shift within compartment B to a smaller E1 value). Lower part of the plot shows the percentage of global bins showing detectable changes. The "A to AwB" category is the most notable but only takes place in 161 bins (~0.5% of all genome bins).

(D) A representative region with ~100 Mb size from chromosome 1 showing largely identical E1 values and largely unaltered A/B compartments between Control and IAA (NUP93 acute depletion) conditions.

(E) Heatmap showing A/B compartment scores of NDGs and NSGs in three Hi-C replicates between Control and IAA (NUP93 acute depletion) conditions. NDGs and NSGs compartment scores (at 100kb resolution) were calculated and ranked by pooling three replicates from the Control condition.

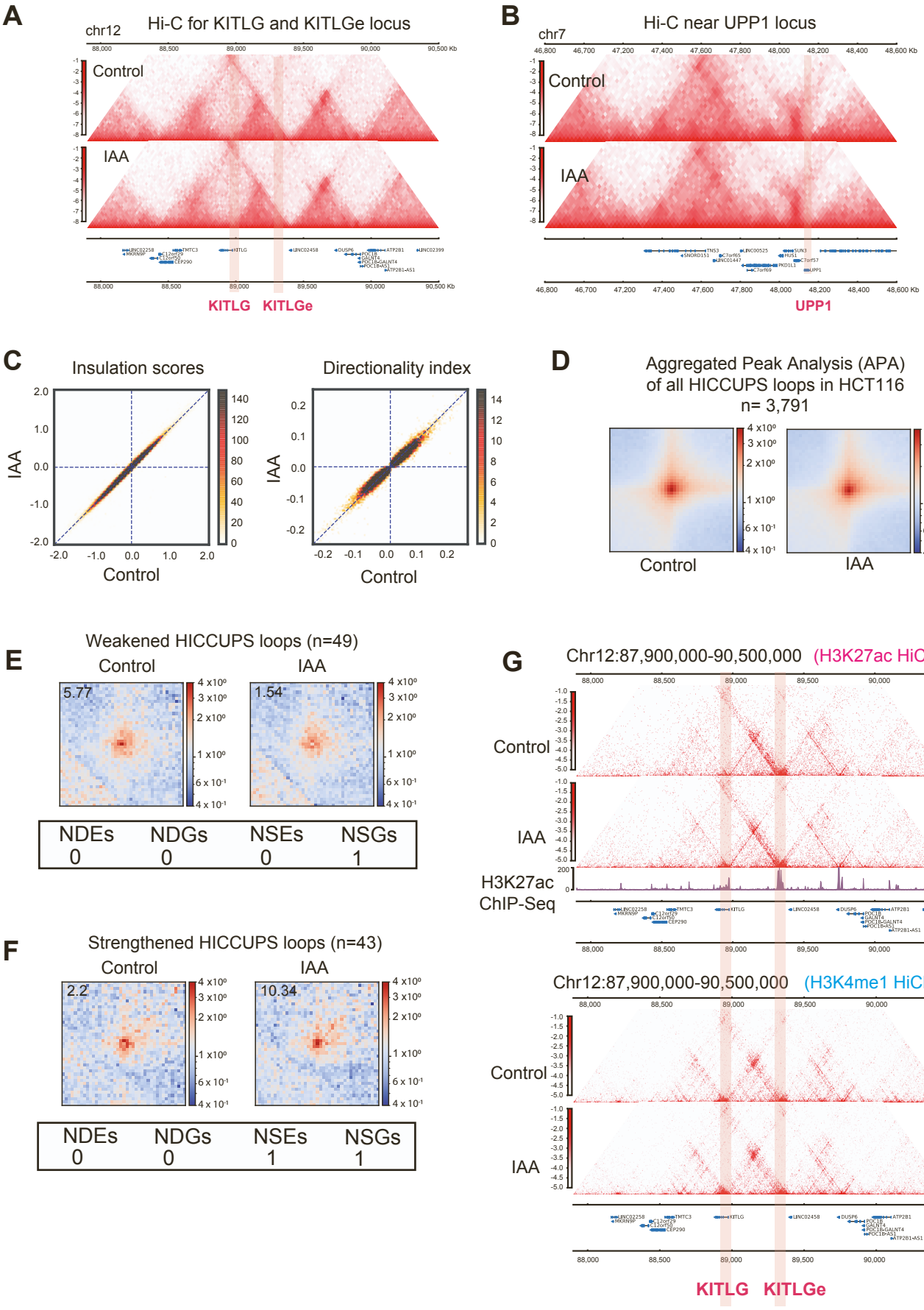
A
chr12
Hi-C for KITLG and KITLGe locus
Control
IAA
KITLG
KITLGe
B
chr7
Hi-C near UPP1 locus
Control
IAA
UPP1
C
Insulation scores
Directionality index
IAA
Control
D
Aggregated Peak Analysis (APA)
of all HICCUPS loops in HCT116
n= 3,791
Control
IAA
E
Weakened HICCUPS loops (n=49)
Control
IAA
5.77
1.54
NDEs 0
NDGs 0
NSEs 0
NSGs 1
F
Strengthened HICCUPS loops (n=43)
Control
IAA
2.2
10.34
NDEs 0
NDGs 0
NSEs 1
NSGs 1
G
Chr12:87,900,000-90,500,000 (H3K27ac HiChIP)
Control
IAA
H3K27ac
ChIP-Seq
Chr12:87,900,000-90,500,000 (H3K4me1 HiChIP)
Control
IAA
KITLG
KITLGe

Figure S7. Additional Hi-C and HiChIP analyses and example regions after NUP93 acute depletion (related to Figure 6).

(A,B) Genome browser snapshots from representative regions encompassing *KITLG* and *KITLG* enhancer (a NDG/NDE locus, chr12:88 Mb to 90.5 Mb), or *UPP1* locus (a NSG, chr7:46.8 Mb to 48.6 Mb), respectively, showing Hi-C contact heatmap in control and 8hr IAA (NUP93 acute depletion) conditions.

(**C**) Scatter plots showing the correlation of Hi-C insulation score or directionality index (two methods to measure TAD boundary strength) in Control (x-axis) or IAA treated (y-axis) conditions. Insulation scores were calculated based on 20kb-binned Hi-C data (Crane et al., 2015). The directionality indexes were also calculated for each 20kb bin.

(D) HICCUPS called 3,791 chromatin loops in HCT116 Hi-C dataset (Rao et al., 2017); the aggregate peak analysis (APA) of Hi-C contacts over these HICCUPS loops showed no difference in the presence or absence of NUP93 (IAA 8hr versus Control).

(E,F) Differential loop analysis of HICCUPS loops identified a few that show quantitative differences by DESeq2 (FDR < 0.05, |log2 (fold change)| >=1). The APA analyses show the heatmaps for the weakened (upper) or strengthened loops (lower) after NUP93 acute depletion. The tables below the heatmaps show the numbers of differential loops (weakened or strengthened) with either of loop anchors overlapping with any NDEs, NDGs, NSEs and NSGs.

(G) HiChIP contact maps from an example region encompassing *KITLG* and *KITLGe* showing overall unaltered chromatin loops in Control and IAA (NUP93 acute depletion) conditions (at 5kb resolution). Top panel is from H3K27ac HiChIP and the bottom is from H3K4me1 HiChIP.

Table S1. A summary of the sequencing datasets generated in this study (related to Figures 1,2,4-7 and Figures S1,S4-S7)

Dataset	Condition	Total Reads	valid contact pairs (for Hi-C or HiChIP)
PRO-seq			
HCT116-NUP93-mAC_UT_PRO-Seq_Rep1	HCT116-NUP93-mAC, PRO-Seq,UT, biological replicate 1	23,492,749	
HCT116-NUP93-mAC_IAA_PRO-Seq_Rep1	HCT116-NUP93-mAC, PRO-Seq, IAA, biological replicate 1	27,864,823	
HCT116-NUP93-mAC_UT_PRO-Seq_Rep2	HCT116-NUP93-mAC, PRO-Seq,UT, biological replicate 2	26,556,805	
HCT116-NUP93-mAC_IAA_PRO-Seq_Rep2	HCT116-NUP93-mAC, PRO-Seq, IAA, biological replicate 2	31,730,919	
ChIP-Seq			
HCT116-NUP93-mAC_UT_H3K27ac_ChIP-Seq	HCT116-NUP93-mAC,ChIP-Seq,H3K27ac,UT	16,824,405	
HCT116-NUP93-mAC_IAA_H3K27ac_ChIP-Seq	HCT116-NUP93-mAC,ChIP-Seq,H3K27ac,IAA	14,441,706	
HCT116-NUP93-mAC_UT_Ser2p_ChIP-Seq_Rep1	HCT116-NUP93-mAC,ChIP-Seq,Ser2p,UT,biological replicate 1	19,849,483	
HCT116-NUP93-mAC_IAA_Ser2p_ChIP-Seq_Rep1	HCT116-NUP93-mAC,ChIP-Seq,Ser2p,IAA,biological replicate 1	24,326,010	
HCT116-NUP93-mAC_UT_Ser2p_ChIP-Seq_Rep2	HCT116-NUP93-mAC,ChIP-Seq,Ser2p,UT,biological replicate 2	28,519,808	
HCT116-NUP93-mAC_IAA_Ser2p_ChIP-Seq_Rep2	HCT116-NUP93-mAC,ChIP-Seq,Ser2p,IAA,biological replicate 2	23,578,265	
HCT116-NUP93-mAC_UT_Pol2(RPB1)_ChIP-Seq	HCT116-NUP93-mAC,ChIP-Seq,RPB1,UT	23,097,338	
HCT116-NUP93-mAC_IAA_Pol2(RPB1)_ChIP-Seq	HCT116-NUP93-mAC,ChIP-Seq,RPB1,IAA	17,318,986	
HCT116-NUP93-mAC_UT_Pol2(RPB2)_ChIP-Seq	HCT116-NUP93-mAC,ChIP-Seq,RPB2,UT	8,619,975	
HCT116-NUP93-mAC_IAA_Pol2(RPB2)_ChIP-Seq	HCT116-NUP93-mAC,ChIP-Seq,RPB2,IAA	10,790,890	
HCT116-NUP93-mAC_UT_BRD4_ChIP	HCT116-NUP93-mAC,ChIP-Seq,BRD4,UT	23,793,283	
HCT116-NUP93-mAC_IAA_BRD4_ChIP	HCT116-NUP93-mAC,ChIP-Seq,BRD4,IAA	25,921,989	
Cut &Run			
HCT116_NUP93_Cut&Run_Rep1	HCT116,Cut&Run,NUP93, biological replicate 1	19,800,662	
HCT116_NUP93_Cut&Run_Rep2	HCT116,Cut&Run,NUP93, biological replicate 2	20,719,390	
HCT116_BRD4_Cut&Run_Rep1	HCT116,Cut&Run for BRD4, biological replicate 1	16,561,482	
HCT116_BRD4_Cut&Run_Rep2	HCT116,Cut&Run for BRD4, biological replicate 2	11,260,577	
HCT116_NUP205_Cut&Run	HCT116,Cut&Run,NUP205	12,098,992	
HCT116_Sec13_CuT&Run	HCT116,Cut&Run,SEC13	12,567,316	
HCT116_NUP35_Cut&Run	HCT116,Cut&Run,NUP35	16,222,422	
HCT116_IgG_Cut&Run	HCT116,Cut&Run,IgG	11,965,322	
HeLa_NUP93_Cut&Run	HeLa,Cut&Run,NUP93	33,149,999	
Hi-C/HiChIP			
HCT116-NUP93-mAC-UT Hi-C rep1	HCT116-NUP93-mAC,Hi-C,MboI,UT,biological replicate 1	193,416,649	95,059,017
HCT116-NUP93-mAC-IAA Hi-C rep1	HCT116-NUP93-mAC,Hi-C,MboI,IAA,biological replicate 1	234,572,997	103,380,686
HCT116-NUP93-mAC-UT Hi-C rep2	HCT116-NUP93-mAC,Hi-C,MboI,UT,biological replicate 2	197,663,263	118,362,751
HCT116-NUP93-mAC-IAA Hi-C rep2	HCT116-NUP93-mAC,Hi-C,MboI,IAA,biological replicate 2	222,252,057	133,835,607
HCT116-NUP93-mAC-UT Hi-C rep3	HCT116-NUP93-mAC,Hi-C,MboI,UT,biological replicate 3	186,653,098	113,750,710
HCT116-NUP93-mAC-IAA Hi-C rep3	HCT116-NUP93-mAC,Hi-C,MboI,IAA,biological replicate 3	209,111,449	127,515,700
HCT116 H3K27ac HiChIP	HCT116,HiChIP, MboI, H3K27ac	156,156,541	52,592,515
HCT116 H3K27ac HiChIP NUP93-mAC-UT rep1	HCT116-NUP93-mAC,HiChIP, MboI, H3K27ac,UT, biological replicate 1	60,443,003	18,209,224
HCT116 H3K27ac HiChIP NUP93-mAC-UT rep2	HCT116-NUP93-mAC,HiChIP, MboI, H3K27ac,UT, biological replicate 2	25,731,156	11,254,815
HCT116 H3K27ac HiChIP NUP93-mAC-IAA rep1	HCT116-NUP93-mAC,HiChIP, MboI, H3K27ac,IAA, biological replicate 1	57,833,324	19,398,729
HCT116 H3K27ac HiChIP NUP93-mAC-IAA rep2	HCT116-NUP93-mAC,HiChIP, MboI, H3K27ac,IAA, biological replicate 2	34,049,952	13,627,953
HCT116 H3K4me1 HiChIP NUP93-mAC-UT rep1	HCT116-NUP93-mAC,HiChIP, MboI, H3K4me1,UT, biological replicate 1	173,570,216	54,949,038
HCT116 H3K4me1 HiChIP NUP93-mAC-IAA rep1	HCT116-NUP93-mAC,HiChIP, MboI, H3K4me1,IAA, biological replicate 1	168,251,826	59,841,587

Table S2. public datasets (related to Figures 1,2,4 and Figures S1,S4 and S7)

Cell line	ChIP-Seq or Hi-C	Accession ID (SRA or 4DN)
HCT116	H3K4me3	SRR6164280
	H3K4me1	SRR6164282
	H3K27me3	SRR6164286
	H3K9me3	SRR6164288
	H3K27ac	SRR6164278
	H3K36me3	SRR6164284
	H3K79me2	SRR5832835,SRR5832836
	H4K20me3	SRR6164294
	CTCF	SRR6164262,SRR6164263,SRR6164264,SRR6164265
	NIPBL	SRR6164298,SRR6164299,SRR6164300,SRR6164301
	RAD21	SRR6164246,SRR6164247,SRR6164248,SRR6164249
	SMC1	SRR6164254,SRR6164255,SRR6164256,SRR6164257
	BRD4	SRR3159130
	P300	SRR1002901,SRR1002902
	pol2	SRR3159128
	ser2p	SRR9106171
	ser5p	SRR9106170
HeLa	P300	SRR502388,SRR502389
	BRD4	SRR1016020
	ser2p	SRR11829925
	pol2	SRR7607778
	H3K27ac	SRR2002376,SRR2002380
HCT116	Hi-C	4DNFIP71EWXC

Table S4. Oligos sequence information (related to Figures 2,3 and Figures S3,S4)

Used for	Name	Sequence	
RT-qPCR primers	GAPDH-mRNA-F	CCTGTTCGACAGTCAGCCGCATC	
	GAPDH-mRNA-R	GGTGACCAGGCGCCCAATACG	
	CCAT1-L-qF	CCACGTGCACATATTTGAATTG	
	CCAT1-L-qR	TGCATTCCCTGCTTAATACTCA	(Jian-Feng Xiang 2014, Cell research)
	MYC-mRNA-qF:	TTGGCAGCAGGATAGTCCTT	
	MYC-mRNA-qR:	TGGTGCTCCATGAGGAGACA	(Jian-Feng Xiang 2014, Cell research)
	KITLG-mRNA-F:	CTTAAACTCCCAGCCCCTGT	
	KITLG-mRNA-R:	TATGCTGCTTTCAGGGTTGTT	
	KITLG-eRNA-F:	TTTCTCCCACTGCAGCTTTT	
	KITLG-eRNA-R:	TGAAGGGGAAGAGAAGCAAA	
	BAHCC1-eRNA-F:	CGCCTTGTCCTGCGTCCC 3	
	BAHCC1-eRNA-R:	ATTTCCCGCCTGCCTGAGTC	
	KMT2D-e-S-F1:	ATTCCATACCCTTGCAGTCGT	
	KMT2D-e-S-R1:	CCAATCTCCTGGCTCTTCTTC	
	SDSL-mRNA-F:	GGTAAAGGCGTATTGGGAGTG	
	SDSL-mRNA-R:	GTCACCTGAGGAGCACACCA	
	UPP1-mRNA-F:	GCAGTGACTGGACAAGGGAACT	
	UPP1-mRNA-R:	GAATCCAACCCCGTTTGTAGAA	
	CCNG2-mRNA-F:	TTGCTATATGGGTGCCAAGA	
	CCNG2-mRNA-R:	GCCCCATTCTTATGGCTGTA	
	FTO-mRNA-F:	AATCTGGTGGACAGGTCAGC	
	FTO-mRNA-R:	TGCCTTCGAGATGAGAGTCA	
Crispr-Cas9 Knock in guide-RNA cloning sequence	Px459_NUP93_gRNA-mAID-F:	CACCGTGCCATGCTTTGTGGGAGTC	
	Px459_NUP93_gRNA-mAID-R:	AAACGACTCCCACAAAGCATGGCAC	
	Px459_NUP35_gRNA-mAID-F:	CACCGAAAGCAATGGAGTACATGTT	
	Px459_NUP35_gRNA-mAID-R:	AAACAACATGTACTCCATTGCTTTC	
Crispr-tethering guide-RNA cloning sequence	HCT-KITLG-promoter-gRNA-F:	CACCGCCCTGCAGCTACTGCTCGCG	
	HCT-KITLG-promoter-gRNA-R:	AAACCGCGAGCAGTAGCTGCAGGGC	
	HCT-KITLG-enhancer-gRNA-F:	CACCGAGCAACTCAAAATACTCGTT	
	HCT-KITLG-enhancer-gRNA-R:	AAACAACGAGTATTTTGAGTTGCTC	
	HCT-CCAT1-(MYC-enhancer)-gRNA-F:	CACCGCATCTCAACAAAAATAAGAT	
	HCT-CCAT1-(MYC-enhancer)-gRNA-R:	AAACATCTTATTTTTGTTGAGATGC	
	HCT-UPP1-promoter-gRNA-F	CACCGGGGCCGGACCTGCCTGCCCC	
	HCT-UPP1-promoter-gRNA-R	AAACGGGGCAGGCAGGTCCGGCCCC	
	HCT-SDSL-promoter-gRNA-F	CACCGAGACCTAAAATGAGAAGACA	
	HCT-SDSL-promoter-gRNA-R	AAACTGTCTTCTCATTTTAGGTCTC	
	HCT-KMT2D-enhancer-gRNA-F	CACCGCCGAACAGGAGGCGGAGGGG	
	HCT-KMT2D-enhancer-gRNA-R	AAACCCCCTCCGCCTCCTGTTCGGC	
	HCT-BAHCC1-enhancer-gRNA-F	CACCGCTCCTGAAAAAAGCAATTAC	
	HCT-BAHCC1-enhancer-gRNA-R	AAACGTAATTGCTTTTTTCAGGAGC	
Primer or sequence for cloning	2XHA pMK291-F:	GTACAAGTTATCCATATGATGTTCCAGATTATGCTTATCCATATGATGTTCCAGATTATGCTT	
	2XHA pMK291-R:	GTACAAGCATAATCTGGAACATCATATGGATAAGCATAATCTGGAACATCATATGGATAACTT	
	NUP35-donor-Fragment1-F:	TGTCTCCTACTGACTAGCCAAGT	
	NUP35-donor-Fragment2-R:	CAGTATGGGTGACACAGCAAG	
	NUP35-donor-Fragment1+2-F:	TGGAGTACATGTTTGGCTGGGGATCCTAGAACACCAAGAAGGAGGT	
	NUP35-donor-Fragment1+2-R:	ACCTCCTTCTTGGTGTTCTAGGATCCCCAGCCAAACATGTACTCCA	
	NUP35-donor-Fragment1-F:	ATCCTTTTACTTGAACATCCCTA	
	NUP35-donor-Fragment2-R:	ACCACTGCCCACTGTCTCAA	
	NUP35-donor-Fragment1+2-F:	AGATGGAGGTCCTCATGAATGGATCCGTCGGCACACTGTCAGTACA	
	NUP35-donor-Fragment1+2-R:	TGTACTGACAGTGTGCCGACGGATCCATTCATGAGGACCTCCATCT	